CONF - 831C143 - -65

AGING DEGRADATION OF CAST STAINLESS STEEL: STATUS AND PROGRAM*

by

CONF-8310143--65

DE84 004018

O. K. Chopra and G. Ayrault

Materials Science and Technology Division
Argonne National Laboratory
Argonne, Illinois 60439

October 1983

To be presented at the 11th Water Reactor Safety Research Information Meeting, October 24-28, 1983, National Bureau of Standards (NBS), Gaithersburg, MD.

*Work supported by the Office of Nuclear Regulatory Research, U.S. Nuclear Regulatory Commission.

AGING DEGRADATION OF CAST STAINLESS STEEL: STATUS AND PROGRAM*

by

O. K. Chopra and G. Ayrault

Materials Science and Technology Division
Argonne National Laboratory
Argonne, Illinois 60439

Abstract

A program has been initiated to investigate the significance of in-service embrittlement of cast duplex stainless steels under light-water reactor operating conditions. The existing data are reviewed to determine the critical parameters that control the aging behavior and to define the objectives and scope of the investigation. The test matrices for microstructural studies and mechanical property measurements are presented. The initial experimental effort is focussed on characterizing the microstructure of long-term, low-temperature aged material. Specimens from three heats of cast CF-8 and CF-8M stainless steel aged for up to 70,000 h at 300, 350, and 400°C were obtained from George Fisher Ltd., of Switzerland. Initial analyses reveal the formation of three different types of precipitates which are not α'. An FCC phase, similar to the $M_{23}C_6$ precipitates, was present in all the long-term aged material.

1. Introduction

Cast duplex stainless steels are used extensively in the nuclear industry to fabricate pump casings and valve bodies for light-water reactors (LWRs) and primary coolant piping in pressurized water reactors (PWRs). The ferrite phase in the duplex structure of austenitic-ferritic stainless steel increases the tensile strength and improves weldability, resistance to stress corrosion, and soundness of castings of these steels. However, the presence of ferrite in these steels introduces several disadvantages regarding their metallurgical stability. Various carbides, brittle chromium-rich phases such as sigma and chi phase, and a chromium-rich BCC phase (α') can precipitate in the ferrite phase or along ferrite/austenite grain boundaries during aging at elevated temperatures. The precipitation of additional phases within the ferrite phase leads to variability in properties, and a reduction in low-temperature ductility due to a phenomenon known as "475°C embrittlement," which is associated with the temperature of maximum embrittlement.

Perhaps the most deleterious phase to form in duplex stainless steel is sigma phase. The presence of molybdenum, and to a lesser extent nickel, in the α phase stabilizes the σ phase and allows it to form at temperatures up to 950°C. Consequently, the cast duplex stainless steels must be cooled past 890°C

---

*Work supported by the Office of Nuclear Regulatory Research, U.S. Nuclear Regulatory Commission.

in less than 2 to 3 min. to avoid the formation of σ phase. Since this phase greatly reduces toughness, it is important to avoid its formation during material processing or elevated-temperature service. The time-temperature curves[1] for various phases and impact strengths of Fe-Cr-Ni alloys, Fig. 1, indicate that embrittlement can be divided into two temperature regimes. At temperatures above 550°C, the embrittlement is largely due to formation of σ phase, and below 500°C the precipitation of α' leads to embrittlement. Formation of carbides and the χ phase can influence mechanical properties in the 500-650°C temperature range; however, the individual effects of carbides and the χ phase, separate from those of σ and α' phases, have not been established.

Experimental data on the aging behavior of ferritic or austenitic/ferritic stainless steel show no evidence of σ-phase formation at temperatures below ~540°C, except in severely cold-worked material where σ is observed at temperatures as low as 482°C. Consequently, σ-phase precipitation is not a concern at the operating temperatures of LWRs, i.e., 288 to 316°C. At these temperatures, embrittlement of ferritic or duplex stainless steels appears to be caused primarily by α' precipitation. The influence of carbides/nitrides on the kinetics of the precipitation process and on the subsequent embrittlement of the material cannot be established from the existing experimental data.

Thermal aging of cast duplex stainless steels at temperatures between 300 and 450°C affects the mechanical properties in several ways.[2-6] In general, thermal aging causes an increase in hardness and tensile strength and a decrease in ductility, Charpy impact strength, and J_{IC} fracture toughness of the material. However, the low-cycle fatigue properties and fatigue crack propagation rates are not significantly modified by aging.[4,5] The changes in the tensile strength and room-temperature impact energy for cast CF-8M stainless steel aged for 3000 h at 427°C are shown in Figs. 2 and 3, respectively. The impact strength, in particular, is reduced by ~80%. Substantial reductions in impact strength have also been observed for several cast CF-8 and CF-8M stainless steels after aging for 10,000 to 70,000 h at temperatures as low as 300°C.[2] The ferrite content of the cast structure has a pronounced influence on the embrittlement behavior, viz., an increase in ferrite content increases the susceptibility to embrittlement, as shown in Fig. 4. Also, addition of molybdenum to the steel, e.g., cast CF-8M, increases both the rate and extent of embrittlement. The very limited data available on J_{IC} fracture toughness also indicate significant reduction in fracture toughness due to low-temperature aging, although the results do not always show good correlation with the trends indicated by the Charpy data.[5]

The kinetics of embrittlement are evaluated by considering the aging phenomenon to be a thermally activated process expressed by an Arrhenius relation. The activation energy is determined by examining the degree of embrittlement (e.g., Charpy impact strength measured at room temperature) produced by different time-temperature histories. In the temperature range of 300 to 400°C, the data obtained by George Fisher, Ltd., of Switzerland[2] for thermal aging of various cast duplex stainless steels yields an activation energy of 100.4 kJ/mole (24,000 cal/mole) for the onset of embrittlement. Figure 4 shows the impact energy of the different cast materials expressed as a function of an aging parameter,[2] P, which represents the degree of aging reached after 10^P h at 400°C. Arrhenius extrapolation can be used to determine the equivalent aging time at other temperatures:

$$t = 10^{P} \exp \frac{U}{R}\frac{1}{T} - \frac{1}{673} , \quad (1)$$

where U is the activation energy, R the gas constant, and T the absolute temperature. For example, a service life of 40 yr at 288 or 316°C, respectively, is equivalent to 10,000 or 28,000 h of aging at 400°C. After the service life at 316°C, the impact energy will be ~12 J for cast materials with ~40% ferrite and ~28 J for castings containing ~14% ferrite.[2]

Recent investigations[5] have described the activation energy for the process of embrittlement as a function of chemical composition of the cast material, given by the relationship

$$Q(\text{kJ/mole}) = -182.6 + 19.9(\%\ \text{Si}) + 11.08(\%\ \text{Cr}) + 14.4(\%\ \text{Mo}). \quad (2)$$

The chemical compositions of the various cast materials used by George Fisher, Ltd. yield activation energies between 65 and 90 kJ/mole (~15 and 22 kcal/mole) for cast CF-8 stainless steels and between 75 and 105 kJ/mole (~18 and 25 kcal/mole) for cast CF-8M stainless steel.

The validity of such an approach for predicting the long-term embrittlement of steels at reactor operating temperatures requires a satisfactory understanding of the aging process and the mechanism of embrittlement to ensure that the activation energy obtained from the laboratory tests is representative of the actual process. The value of activation energy determined from the aging data for cast duplex stainless steels is much lower than that expected for a mechanism controlled by solute bulk diffusion (i.e., activation energy of 54,900 cal/mole). These results indicate that the precipitation of α' occurs not via nucleation and growth but by another mechanism, e.g., spinodal decomposition, or that processes other than α' precipitation contribute to embrittlement. The available information on the microstructure of aged cast duplex stainless steels is not sufficient for correlating the microstructure with the mechanical properties or for determining the mechanism of low-temperature embrittlement.

Changes in the composition of the ferrite phase in cast duplex steels also influence the aging behavior and add to the uncertainty of predicting the long-term embrittlement behavior. The extensive information on the embrittlement of single-phase binary Fe-Cr ferritic alloys is helpful in gaining insight into the effects of composition on aging and in identifying possible mechanisms of embrittlement. Unfortunately, the bulk of this work has been carried out at temperatures of 400°C or above, and caution must be observed in extrapolating to reactor temperatures. Data on the thermal aging of single-phase ferritic alloys indicate that an increase in chromium, molybdenum, or titanium content in the ferrite phase decreases the time required for embrittlement.[7] The influence of chromium is more pronounced than that of molybdenum or titanium. Variations in manganese or silicon content have no effect on the aging behavior.[8] For single-phase Fe-Cr-Ni alloys, an increase in the nickel content promotes α' precipitation[8] but the higher nickel ferritic steels take longer to embrittle because other deformation modes, such as twinning, are promoted by additions of nickel.[9] Interstitial elements such as carbon and nitrogen also accelerate embrittlement of single-phase ferritic steels. Nitrogen in the ferrite phase influences the aging behavior by enhancing the precipitation of the α' phase and by the formation of nitrides or carbonitrides.[7,10-12]

2. Program Scope

The objectives of this program are to (1) characterize and correlate the microstructure of in-service reactor components and laboratory-aged material with loss of fracture toughness and identify the mechanism of embrittlement, (2) determine the validity of laboratory-induced embrittlement data for predicting the toughness of component materials after long-term aging at reactor operating temperatures, (3) characterize the loss of fracture toughness in terms of fracture mechanics parameters in order to provide the data needed to assess the safety significance of embrittlement, and (4) provide additional understanding of the effects of key compositional and metallurgical variables on the kinetics and degree of embrittlement.

Material was obtained from various experimental and commercial heats of ASTM A351 and A451 grades of CF-8, -8M, and -3 cast stainless steel in different product forms and section thicknesses. Nineteen experimental heats of stainless steel cast material were obtained in the form of keel blocks. The composition was varied to provide different concentrations of nickel, chromium, carbon, and nitrogen in the material and ferrite contents in the range of 3 to 30%. Sections from five different centrifugally cast pipes (grades CF-8 and CF-8M), a pump impeller, and a pump casing (grade CF-8) were also procured. The OD and wall thickness of the cast pipes range from 0.6 to 0.9 m and 38.1 to 76.2 mm, respectively. Material will be available for Charpy-impact tests and microstructural studies over the entire range of compositions. However, it is prohibitively expensive to procure and age material for J_R curve testing for all compositions. A more restricted set of compositions was selected for these tests. The material will be obtained from large heats (∿2000 lb) in the form of 76-mm-thick slabs.

The test matrix for the microstructural studies and mechanical property measurements is given in Table 1. Since different amounts of material will be available from the various sources, the actual tests performed on the material will vary. The time and temperature for aging of the cast material for the different mechanical tests are given in Table 2. The relationships of time and temperature to the initiation of precipitation and the onset of embrittlement will be determined by microstructural examination, hardness measurements, and Charpy-impact tests. Measurements of impact strength and ductile-to-brittle transition temperature (DBTT) will be used to define the aging histories, chemical compositions, and metallurgical structures that lead to significant embrittlement and to better characterize the embrittlement phenomenon. Measurements of fracture toughness will be carried out to determine the degree of embrittlement that can be expected as a function of service time and the compositional variables.

The initial experimental effort is focussed on microstructural studies on cast duplex stainless steel aged in the laboratory at low temperatures for long times. The microstructures observed in these experiments will be compared with those obtained from materials aged in service at reactor operating temperatures. Twenty fractured impact bars from three heats of aged cast duplex stainless steel (grades CF-8 and CF-8M) were obtained from George Fisher, Ltd. The material was used earlier to study the long-term aging behavior of cast stainless steels.[2] The specimens from CF-8 cast stainless steel (heats 278 and 280) were aged for 3000, 10,000, and 70,000 h at 300, 350, and 400°C, while the specimens from CF-8M stainless steel (heat 286) were aged for 1000 and 10,000 h at 400°C.

Two ferritic alloys, heats 26Cr-1Mo and 29Cr-4Mo-2Ni, and a cast duplex stainless steel (heat B) were used to develop the technique for preparing transmission electron microscope (TEM) samples from the cast materials. The ferritic alloys were supplied by Allegheny Ludlum Steel Corp., and have been used in a study of the "475°C embrittlement" phenomenon at temperatures between 371 and 593°C.[13] Material from the two ferritic alloys and cast stainless steel (heat B) was aged for 100 and 1000 h at 400 and 475°C for TEM inspection.

3. Microstructural Evaluation

Aging of the cast CF-8 stainless steel, heat B, for 1000 h at 475°C produced two different types of precipitates in the ferrite grains. A general precipitate was distributed uniformly in the ferrite grain; another was found only on dislocations. Neither of the precipitates were present in the unaged specimens. The general precipitate had a mottled or "orange peel" appearance in bright-field images, Fig. 5a, but produced no detectable changes in diffraction patterns. Such micrographs are generally accepted as evidence of the chromium-rich α' precipitates. The mottled-contrast images seen in duplex stainless steel and Fe-46Cr alloy were shown (by Mossbauer spectroscopy[8] and precipitate extraction techniques,[9] respectively) to be due to α'. The precipitates formed on the dislocations, Fig. 5b, were typically 15- to 40-nm cubes with {100} matrix planes as faces. These precipitates were not α' and exhibited a distinct diffraction pattern consistent with a FCC structure similar to $M_{23}C_6$ patterns, but with a slightly larger lattice parameter. The precipitates also had a cube-on-cube orientation relative to the BCC ferrite matrix, which would be unusual for $M_{23}C_6$ phase. Preliminary energy-dispersive X-ray analyses indicated an enrichment of Ni and Si in these precipitates. These results suggest that the precipitates are probably G-phase (a phase rich in Ni and Si), which has been observed in Fe-12Cr-4Ni alloy after aging at 450°C[14] and in commercial EM-12 (9Cr-2Mo), HT-9 (12Cr-1Mo), and AISI 416 (13Cr) ferritic steels after irradiation at temperatures <425°C.[15] Until a more positive identification can be made, these precipitates will be designated as $M_{23}C_6$-like precipitates.

Aging of the two single-phase ferritic alloys, heats 26Cr-1Mo and 29Cr-4Mo-2Ni, for 1000 h at 475°C also produced the mottled bright-field images associated with the α' precipitates. In addition, platelet precipitates were observed in the 29Cr-4Mo-2Ni alloy. The precipitate microstructure of the ferritic alloys is essentially identical to that reported in an earlier study.[13] The diffraction patterns and the contrast images of the platelets suggest that they are not α' or the $M_{23}C_6$-like precipitates.

Aging for 1000 h at 400°C produced no obvious microstructural change in CF-8 cast stainless steel and 26Cr-1Mo ferritic alloy. Platelet precipitates were observed in the 29Cr-4Mo-2Ni ferritic alloy.

TEM examination of the aged cast duplex stainless steel specimens obtained from George Fisher, Ltd. did not reveal the mottled images of α' precipitates. The CF-8 stainless steel, heat 280 (containing 40% ferrite), aged for 66,650 h at 400°C, underwent profuse precipitation in the ferrite grains, both at and away from dislocations, as shown in the images in Fig. 6. These precipitates were similar to the $M_{23}C_6$-like precipitates observed in heat B which was aged for 1000 h at 475°C. Precipitates that formed on the dislocations were about 15 nm in diameter and those away from dislocations were ∿5 nm in size. The diffraction pattern, shown in Fig. 7, indicates a FCC unit cell with a cube-on-cube orientation with the ferrite matrix. The precipitate unit cell is a factor of about 3.95 larger than that of the ferrite matrix. These precipitates were not present after aging for 10,000 h at 400°C. Another type of precipitate was observed on the dislocations, as shown in Fig. 8. The precipitate, however, could not be identified. The precipitate reflections were too weak owing to a low volume fraction and were streaked as a result of small size. This fine-sized precipitate was the only precipitate present in the specimens of heat 280 aged for 70,000 h at 300°C.

Examination of heat 278 (containing 15% ferrite) of CF-8 cast stainless steel aged for ∿70,000 h at 400°C also revealed the $M_{23}C_6$-like precipitates; however, their distribution was somewhat different than that in heat 280. In heat 278 the precipitates on dislocations tended to be larger whereas those away from dislocations were smaller. Furthermore, it was clear from diffraction pattern intensities of the precipitates that heat 278 had a lower volume fraction of precipitates than heat 280. Heat 278 was found to embrittle more slowly than heat 280 in tests performed by George Fisher, Ltd.[2] The different distribution of precipitate phases suggests that the greater ferrite content is not the only reason for rapid embrittlement of heat 280. The $M_{23}C_6$-like precipitates were also observed in heat 278 after aging for 70,000 h at 300°C, as shown in Fig. 9. This same heat treatment did not produce $M_{23}C_6$-like precipitates in heat 280. These results indicate that small changes in alloy chemistry not only affect the ferrite content but also influence the precipitation behavior.

Microstructural evaluation of aged CF-8M stainless steel also indicates that the embrittlement behavior is related to precipitate morphology and distribution. Data obtained on the long-term aging behavior of cast duplex stainless steels[2] indicate that the loss of impact strength of CF-8M, heat 286, after aging for 10,000 h at 400°C is equivalent to that for the CF-8, heat 280, aged for 66,650 h at 400°C. TEM examination of CF-8M stainless steel, heat 286, aged for 10,000 h at 400°C, revealed profuse intragranular precipitates, both at and away from dislocations, as shown in Fig. 10. The degree of precipitation in the CF-8M specimen is comparable to that in heat 280 aged for 66,650 h at 400°C and much greater than that in heat 278 aged for 66,650 h at 400°C. Diffraction patterns of the specimen show the $M_{23}C_6$-like precipitates to be about 3 nm in diameter, as shown in Fig. 10b. However, intense reflections were also observed near the {333} and {115} FCC precipitate reflections, which produced larger (∿5 nm) images at the same sites as the images from the FCC reflections, as shown in Fig. 10c. These larger precipitates form a virtual coating on dislocations and should therefore be effective in dislocation pinning. It is not yet clear whether the larger precipitates simply nucleate at the sites of the smaller precipitates or form by transformation of the FCC precipitate phase. A more detailed inspection of these specimens and the specimens aged at 350°C is in progress.

4. Summary

A program has been initiated to investigate the significance of in-service embrittlement of cast duplex stainless steels under LWR operating conditions. The existing data were reviewed to determine the critical parameters that control the aging behavior and to establish the test matrices for microstructural studies and mechanical property measurements. Various experimental and commercial heats of ASTM A351 and A451 grade of CF-8, -8M, and -3 cast stainless steel were procured in different product forms and section thicknesses. The composition of the experimental heats was varied to provide different concentrations of nickel, chromium, carbon, and nitrogen in the material and ferrite contents in the range of 3 to 30 volume percent. Test specimens are being aged at temperatures of 290, 320, 350, 400, and 450°C and for times ranging from 300 to 50,000 h. Material will be available for Charpy impact tests and microstructural studies over the entire range of compositions. A more restricted set of compositions is selected for J_R-curve testing and DBTT determination. Measurements of impact strength will be used to define the critical parameters that lead to significant embrittlement of the material and to better characterize the phenomenon of embrittlement. Measurements of fracture toughness will be carried out to determine the degree of embrittlement that can be expected under LWR operating conditions.

The initial effort, already begun, is focussed on microstructural characterization of aged specimens of CF-8 and CF-8M cast stainless steel, obtained from George Fisher, Ltd. None of the specimens aged at temperatures between 300 and 400°C exhibited the mottled structure of α' precipitates. Instead, three different types of precipitates were observed in the specimens; an FCC phase (designated $M_{23}C_6$-like precipitate for lack of positive identification) present both on and away from dislocations in all long-term aged specimens, a fine and uniformly distributed precipitate observed in heat 280 of CF-8 stainless steel aged for relatively short times or at low temperature, and a large precipitate observed at the same sites as the $M_{23}C_6$-like precipitate. The $M_{23}C_6$-like precipitate may be G-phase, a phase rich in Ni and Si. The microstructural changes in the aged duplex stainless steels indicate a definite correlation between loss of impact strength and degree of precipitation in these specimens.

References

1. H. D. Solomon and T. M. Devine, "Influence of Microstructure on the Mechanical Properties and Localized Corrosion of a Duplex Stainless Steel," MiCon 78: Optimization of Processing, Properties, and Service Performance Through Microstructural Control, eds. Abrams, Maniar, Nail and Solomon, ASTM STP 672 (1979), p. 430.

2. A. Trautwein and W. Gysel, (a) "Influence of Long Time Aging of CF8 and CF8M Cast Steel at Temperatures Between 300 and 500 Deg. C on the Impact Toughness and the Structure Properties," Spectrum, Technische Mitteilungen aus dem+GF+Konzern, No. 5, May 1981; Stainless Steel Castings, eds. V. G. Behal and A. S. Melilli, ASTM STP 756 (1982), p. 165; (b) Figure in EPRI NP-2705-SR (October 1982), p. 3.18.

3. G. Baudry and C. Pichard, "Evolution During Long Holding Times at 300 and 450°C of the Mechanical Properties of Austeno-Ferritic Steel Castings and Welded Joints Used in Pressurized Water Nuclear Reactors," Troisieme Congres National Sur La Technologie Des Appareils a Bression, Vol. 2, Materiaux, A.F.I.A.P. (1980), p. 673.

4. E. I. Landerman and W. H. Bamford, "Fracture Toughness and Fatigue Characteristics of Centrifugally Cast Type 316 Stainless Steel Pipe after Simulated Thermal Service Conditions, Ductility, and Toughness Considerations in Elevated Temperature Service," ASME MPC-8 (1978), p. 99.

5. G. Slama, P. Petrequin, and T. Magep, "Effect of Aging on Mechanical Properties of Austenitic Stainless Steel Castings and Welds" presented at SMIRT Post-Conference Seminar 6, Assuring Structural Integrity of Steel Reactor Pressure Boundary Components, Monterey, CA. Aug. 29-30, 1983.

6. W. H. Bamford, E. I. Landerman, and E. Diaz, "Thermal Aging of Cast Stainless Steel and Its Impact on Piping Integrity," presented at ASME National Congress on Pressure Vessels and Piping, Portland, Oregon, 1983.

7. P. J. Grobner, "The 885°F (475°C) Embrittlement of Ferritic Stainless Steels," Metall. Trans. 4, 251 (1973).

8. H. D. Solomon and L. M. Levinson, "Mossbauer Effect Study of 475°C Embrittlement of Duplex and Ferritic Stainless Steels," Acta Metall. 26, 492 (1978).

9. M. J. Marcinkowski, R. M. Fisher, and A. Szirmae, "Effect of 500°C Aging on the Deformation Behavior of an Iron-chromium Alloy," Trans. AIME 230, 676 (1964).

10. A. Hendry, Z. F. Mazur, and K. H. Jack, "Influence of Nitrogen on 475°C Embrittlement of High-chromium Ferritic Steels," Met. Sci. 13, 482 (1979).

11. M. Courtnall and F. B. Pickering, "The Effect of Alloying on 475°C Embrittlement," Met. Sci. 10, 273 (1976).

12. R. Lagneborg, "Metallography of the 475°C Embrittlement in an Iron-30% Chromium Alloy," Trans. ASM 60, 67 (1967).

13. T. J. Nichol, A. Dalta, and G. Aggen, "Embrittlement of Ferritic Stainless Steels," Metal. Trans. 11A, 573 (1980).

14. G. T. Brown and R. T. Allsop, "Embrittlement of a 12%Cr-4Ni Steel," J. Iron Steel Inst. (1960), p. 435.

15. D. S. Gelles and L. E. Thomas, "Effects of Neutron Irradiation on Microstructure in Commercial and Experimental Ferritic Alloys," presented at the Topical Conf. on Ferritic Alloys for use in Nuclear Energy Technologies, Snowbird, Utah, June 19-23, 1983.

Table 1. Test Matrix for Cast Material of CF8 and CF8M Stainless Steel

Material	Metallurgical Characterization[a]	TEM & Neutron Diffraction	Charpy Impact	Hardness	Instrumented Impact	DBTT	J_R Curve[b]
Swiss impact specimens	x	x					
In-service components	x	x	x	x			x
Large heats[c]	x		x	x	x	x	x
Reactor components[c]	x	x	x	x	x	x	x
Small heats[c]	x	x	x	x			

[a] Characterization of chemical composition, ferrite content, and grain size and structure.

[b] 2T-compact tension specimens will be used for the large heats and 1T-compact tension specimens will be used for reactor components.

[c] Tests will be performed after thermal aging.

Table 2. Time and Temperature for Aging of the Cast Material for Charpy and Impact and J-Integral Tests

Time, h	Temperature, °C				
	450	400	350	320	290
100	a	a			
300	a	a	a		
1,000	a	a	a	a	
3,000	a	a	a,b	a	a
10,000	a	a,b	a,b,c	a,b	a
30,000	a	a	a,b,c	a,b,c	a,b,c
>50,000		a	a	a,b	a,b

[a] Charpy impact test at room temperature. Experimental heats: 4 specimens each condition; reactor components: 3 axial (A-T) and 2 transverse (T-A) specimens each condition.

[b] Instrument Charpy impact test at room temperature. Experimental heats and reactor components: 2 specimens (A-T) each condition. J-Integral test at room temperature. Reactor components: 2 A-T and 1 T-A specimens each condition.

[c] Charpy impact test at 7 temperatures (DBTT). Reactor components: 14 A-T specimens each condition. J-Integral test at 290°C. Reactor components: 2 A-T specimens each condition.

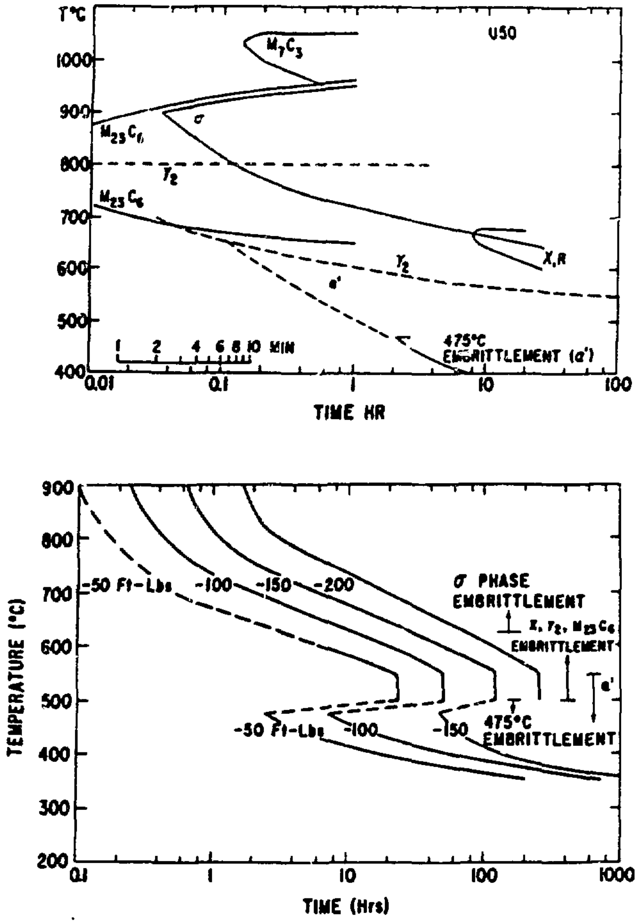

Fig. 1. Time-Temperature Curves for Various Phases and Decrease in Room-Temperature Impact Energy of Cast Duplex Stainless Steel. [Solomon and Devine, Ref. 1]

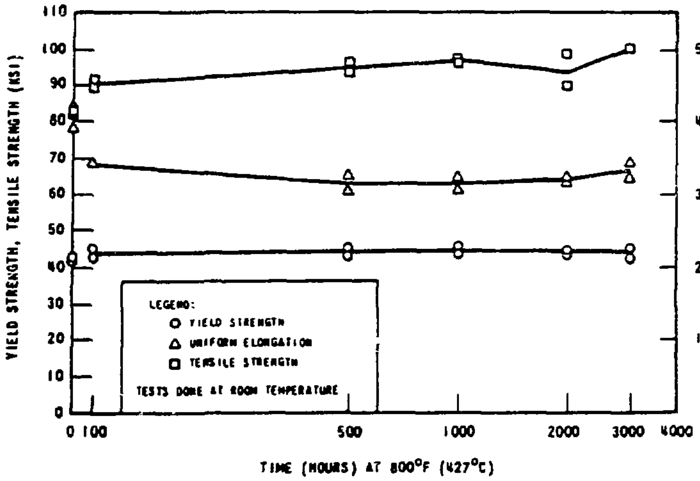

Fig. 2. Increase in Tensile Strength from Low-Temperature Aging of Cast CF-8M Grade A-451 Stainless Steel. [Landermann and Bamford, Ref. 4]

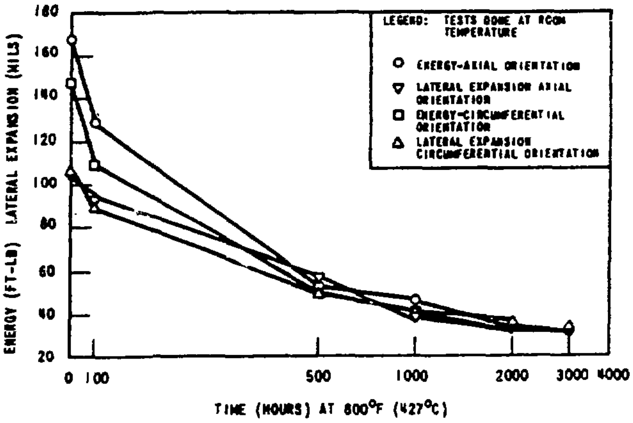

Fig. 3. Decrease in Room-Temperature Impact Energy from 475°C Embrittlement of Cast CF-8 Grade A-451 Stainless Steel. [Landermann and Bamford, Ref. 4]

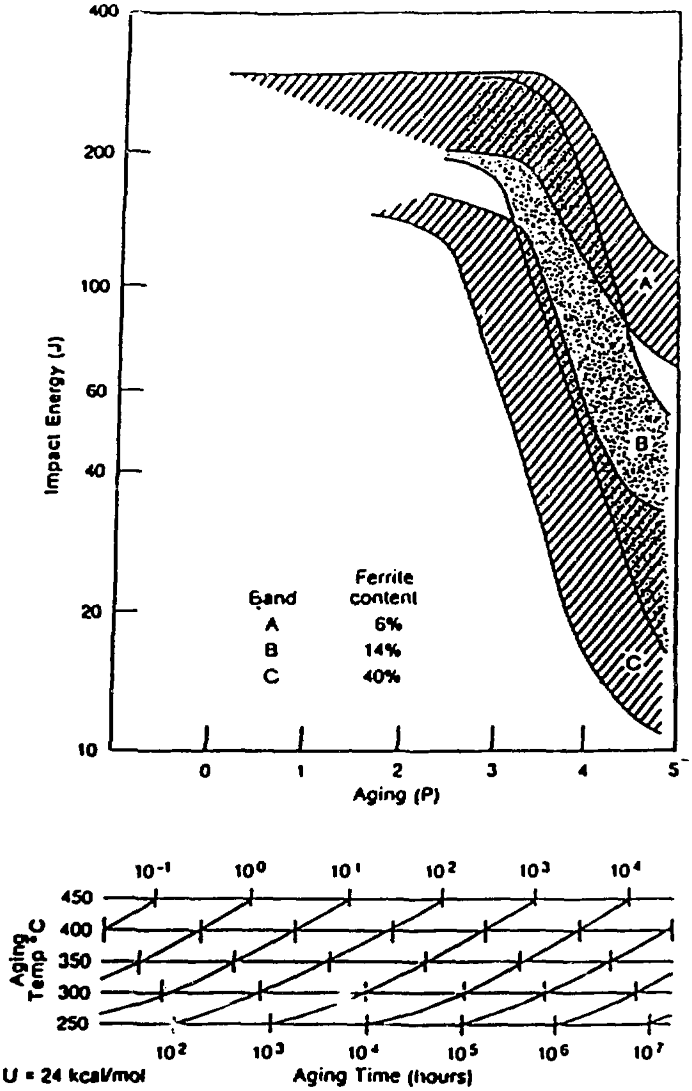

Fig. 4. Influence of Ferrite Content on the Embrittlement of Cast CF-8 and CF-8M Grade A-351 Stainless Steel. [Trautwein and Gysel, Ref. 2b]

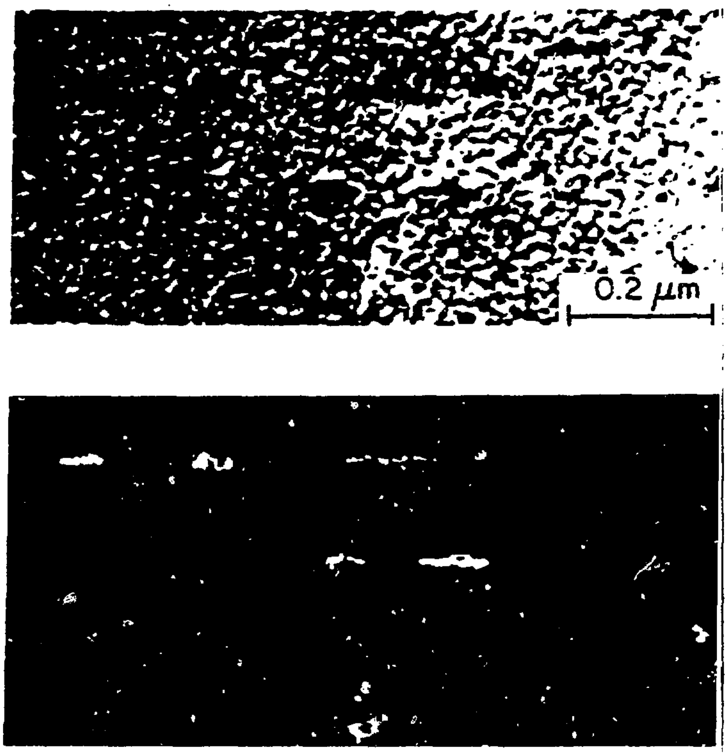

Fig. 5. Precipitation in A351 Cast CF-8 Stainless Steel Aged 1000 h at 475°C. (a) Bright-field image under (110) two-beam diffraction conditions, and (b) dark-field image using (333) reflection in the FCC precipitate diffraction pattern.

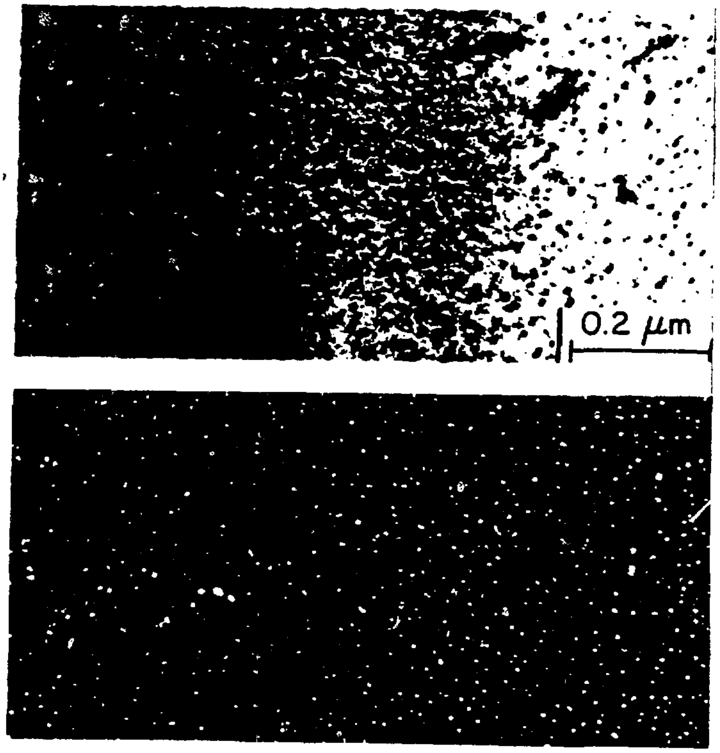

Fig. 6. Bright- and Dark-Field Images of Precipitates in the Ferrite Phase of CR-8 Stainless Steel (Heat 280) Aged for 66,650 h at 400°C.

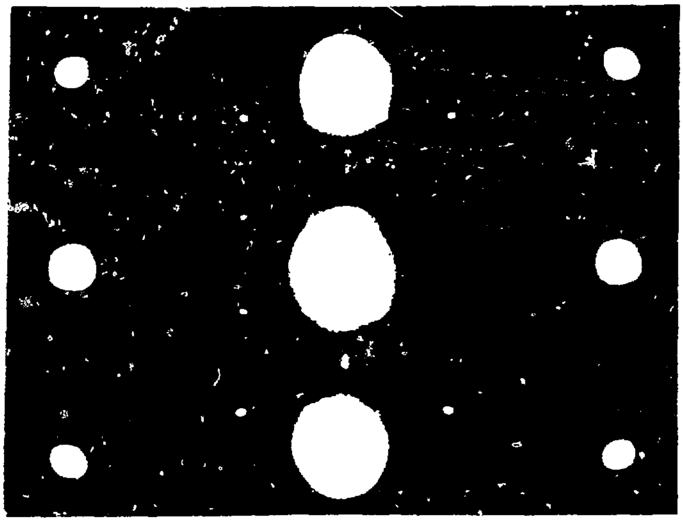

Fig. 7. Selected Area Diffraction Pattern at (110) Orientation in CF-8 Stainless Steel (Heat 280) Aged for 66,650 h at 400°C.

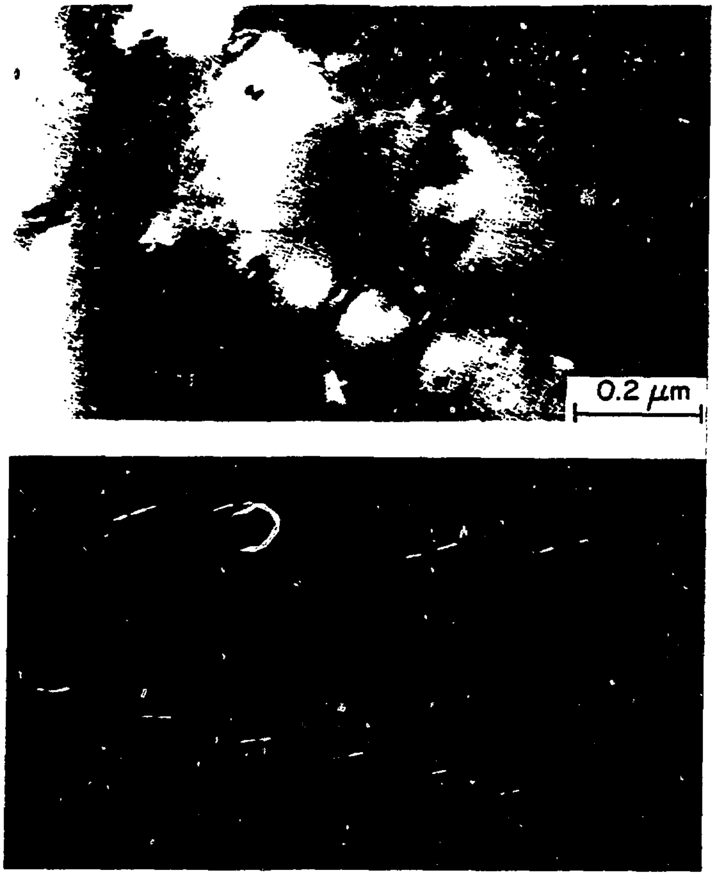

Fig. 8. Bright- and Dark-Field Images of Precipitates in CF-8 Stainless Steel (Heat 280) Aged for 10,000 h at 400°C.

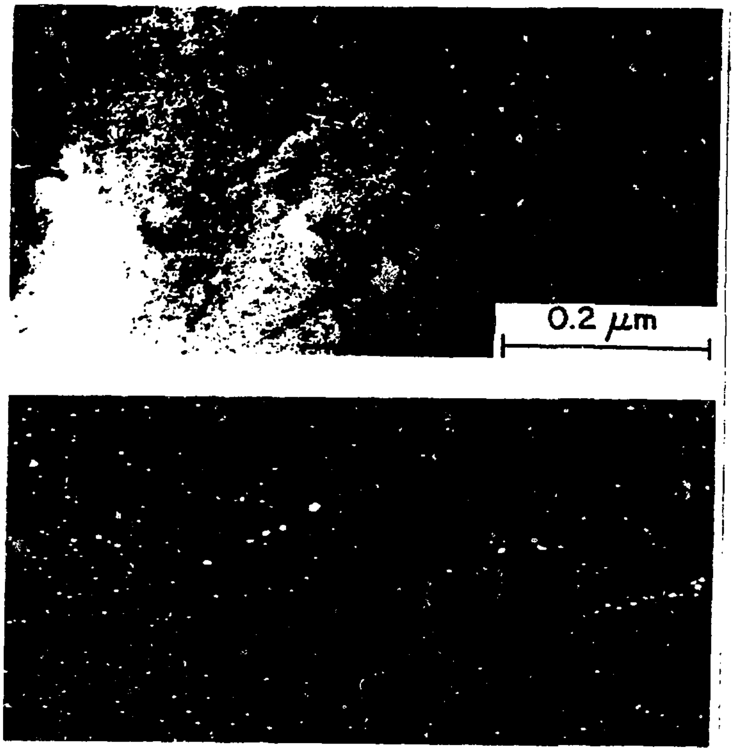

Fig. 9. Bright- and Dark-Field Images of Precipitates in CF-8 Stainless Steel (Heat 278) Aged for 70,000 h at 300°C.

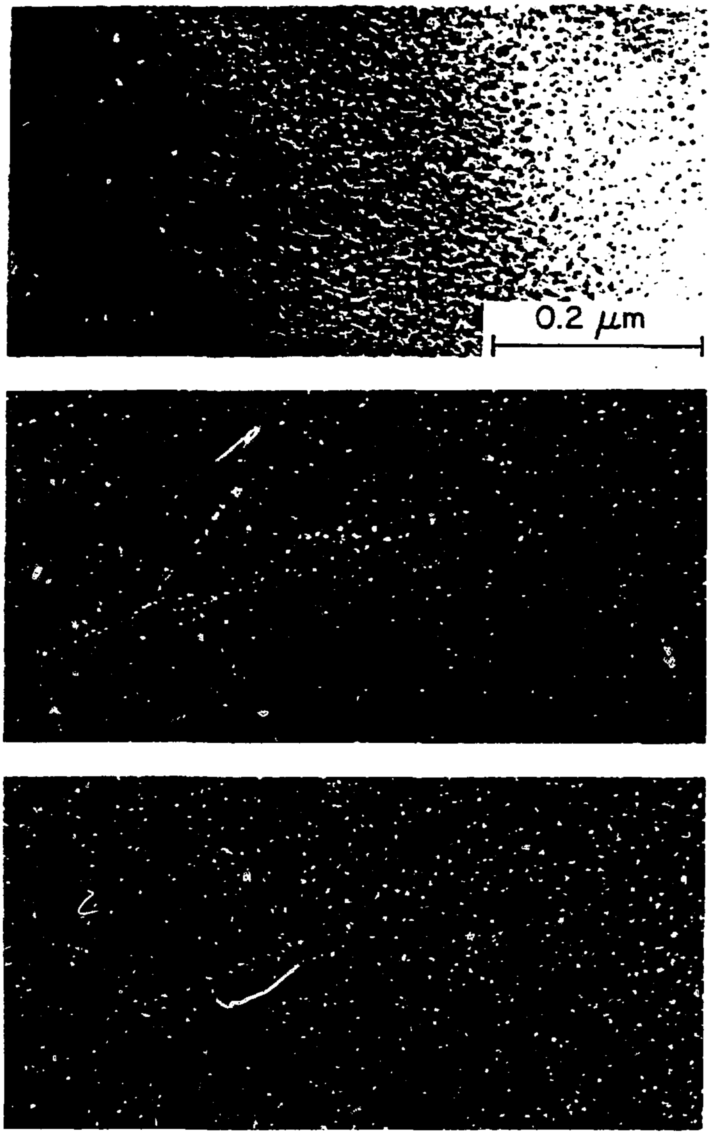

Fig. 10. Precipitates in CF-8M Stainless Steel (Heat 286) Aged for 10,000 h at 400°C. (a) Bright field, (b) dark field using {600} precipitate reflections, and (c) dark field using {115} precipitate reflections.